Active Control of a Cylinder Wake Using Surface Plasma

Timothy JUKES and Kwing-So CHOI

University of Nottingham, Nottingham, NG7 2RD, UK, timothy.jukes@nottingham.ac.uk

Abstract. An experimental investigation has been undertaken using high-speed Particle Image Velocimetry to study the possibility of controlling the global flow field in the near wake of a circular cylinder at Re = 6,500. Surface plasma actuators were mounted at strategic locations around the cylinder (both fore and aft of the separation point) and used for flow control by producing a body force close to the wall. It was found that the plasma can significantly alter the vortex shedding in the wake of the cylinder, with effectiveness depending upon the actuator location and forcing frequency. The most dramatic effects were observed when the plasma was located very close to the natural laminar separation point. Here, amplification of the shedding was observed when the plasma was excited at the natural vortex shedding frequency ($St_f \approx 0.2$, $St_K = 0.206$). This was accompanied by periodic flow reattachment to at least the rearward stagnation point. At higher forcing frequency ($St_f \geq 0.8$), the plasma completely suppressed the vortex shedding process which lead to a short and narrow wake, reduced turbulence intensity, and 60% reduction in the wake momentum thickness. At still higher frequency ($St_f \geq 2.0$, $St_{SL} = 1.7$), only the shear layers were excited and the vortex street remained unaltered.

Key words: flow control, surface plasma, circular cylinder, PIV.

1. Introduction

Flow around circular cylinders is one of the oldest problems in fluid mechanics and has been extensively studied since the late 19th century due to its engineering significance and relative simplicity in experiment. Many review papers have been written on the subject (see, for example, Williamson [17]). The focus of these experiments are within the Transition-in-Shear-Layer (TrSL or subcritical) state of flow [18], which was first examined in detail by Bloor [2]. Within this flow regime, the shear layers initially develop 2D transition waves ($400 < Re <$ 1k - 2k), which then roll-up into discrete vortices that feed into the Kármán vortex street ($2k < Re <$ 20k - 40k). Here $Re = U_\infty d/\nu$ is the Reynolds number, where U_∞ is the free-stream velocity, d is the cylinder diameter and ν is the kinematic viscosity of the fluid. Prasad and Williamson [13] showed that the transition vortices occur at a frequency (normalised with the primary vortex shedding frequency) that varies with $Re^{0.67}$.

An effective method for controlling the cylinder wake is by rotational oscillation of the cylinder about its axis. Tokumaru and Dimotakis [16] studied the flow at $Re = 1.5 \times 10^4$ using a maximum rotational speed, $\Omega = V_{r,max}/U_\infty$, with a forcing Strouhal number, $St_f = fd/U_\infty$, in the range $0 \leq \Omega \leq 16$ and $0.17 \leq St_f \leq 3.3$, where f is the oscillation frequency. Four vortex shedding modes were identified for different values of St_f. When the forcing frequency was similar to

the natural shedding frequency (St_f = 0.2), two vortices of the same sign were released per half cycle. At higher St_f (0.2 – 1), the wake structure became synchronised to the rotational oscillation frequency. At $1.1 \leq St_f \leq 1.5$, the near-wake structure was synchronised but became unstable and developed into a vortex street with lower spatial frequency downstream. For $St_f > 2$, the oscillation only affected the shear layers near the cylinder, with a largely undisturbed vortex street. A broad minimum in drag occurred when $St_f > 0.8$, due to a delay in mean separation and a thinning of the wake. Similar results were reported using DNS [4, 5], although it was noted that the range for eddy shedding lock-on became narrower as Ω was reduced. Small-amplitude oscillations have also been used ($0.005 \leq \Omega \leq 0.03$), which were very effective at exciting the shear layer instability for $St_f > 0.6$ [8].

Surface plasma is an emerging technique for flow control due to its unique ability to create a body force close to the wall in atmospheric pressure air. The actuators are simple, lightweight, require no moving parts and are extremely fast acting. Plasma actuators have been observed to create laminar wall jets accompanied by initiation vortices [9], and have been used to reduce the skin friction drag in turbulent boundary layers by up to 45% [10]. Enloe *et al*. [7] provide details of the plasma formation and Corke and Post [6] presented details of the body force produced by the plasma.

Plasma actuators have proved successful in locking-on the vortex shedding to the forcing frequency over a circular cylinder [11, 12], and synchronising the shedding from two side-by-side cylinders [1]. In addition, Thomas *et al*. [15] observed that the vortex street could be suppressed when $St_f \approx 1$. The wake turbulence was dramatically reduced and a very short, tapered wake region occurred which was much thinner than the canonical case.

The aim of this study is to explore the potential of plasma actuators for dynamic separation control over a circular cylinder. High frame-rate PIV is used to study the dynamics of the near-wake at Re = 6,500. Actuators are placed at several azimuthal locations both fore and aft of the separation point (±70°, 89°, 100°, 130°) with periodic forcing in the range $0.2 \leq St_f \leq 4.0$. Top and bottom actuators are operated in unison and alternately, with both constant forcing duration and constant duty cycle throughout the St_f range.

2. Experimental Arrangement

Experiments were conducted in a low-speed open return wind tunnel with test section of dimensions 1.5 x 0.3 x 0.3m. The circular cylinder consisted of a hollow acrylic tube (d = 50mm) spanning the test section 0.4m downstream of the contraction. Endplates were fitted to the cylinder which extended 5d in the streamwise direction ($-1.5 < x/d < 3.5$) and 3d in the cross-flow direction ($-1.5 < y/d < 1.5$), where the origin is located at the centre of the cylinder. All experiments were conducted at U_∞ = 2m/s (Re = 6,500).

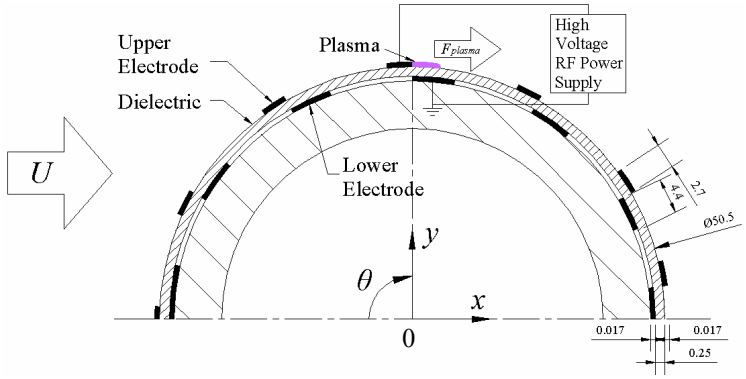

Figure 1. Circular cylinder cross-section. All dimensions in mm. Note the height of the upper electrodes, k, is exaggerated (roughness ratio, $k/d = 3\text{x}10^{-4}$).

The plasma actuators consisted of 17μm thick copper electrodes separated by 250μm thick Mylar dielectric (dielectric constant, $\varepsilon = 3.1$). Several actuators were photochemcially etched onto a single sheet, which was wrapped around the acrylic tube and bonded in place so that they were located at 30° intervals (Fig. 1). Wires were soldered to the electrodes and fed outside the wind tunnel so that the actuators could be used independently or in pairs. In order to create the plasma, a bipolar square waveform was delivered to the upper electrodes with frequency, f_{plasma} = 25kHz, 35% duty cycle, and voltage, E_{plasma} = ±3.5kV. This locally ionized the ambient gas around it, causing plasma to spread out over the surface of the cylinder. This appeared as a light purple glow extending for around 3mm to the side of the electrode under which the lower electrode was placed. In these experiments, plasma was formed only on the downstream edges of the electrodes which caused a body force to be directed in the downstream direction. Details of the plasma characteristics and power supply can be found in [9].

Measurements of the flow field in the near wake were made using a High Frame-Rate Particle Image Velocimetry (PIV) System from TSI. The system consisted of a PowerView HS-3000 high-speed camera, New Wave Research Pegasus PIV laser (45W Nd:YLF), TSI 9307-6 Oil Droplet Generator and a dedicated PC. The laser sheet was aligned along the streamwise direction and at the centreline of the wind tunnel. Olive oil was used to seed the flow with 1μm diameter droplets. Generally, the camera was set to view the cylinder wake in the region $0 < x/d < 2.5$, $-1 < y/d < 1$. Image pairs were then taken at a frame rate of 250Hz (Δt = 300μs between pairs, 10ns laser pulse). Velocity vectors were computed on a 16x16 pixel grid using a recursive cross-correlation technique.

3. Results

3.1. EFFECT OF PLASMA IN STILL AIR

The effect of activating a single plasma actuator in still air is shown in Fig. 2. Plasma was activated for a total of 33.2ms, corresponding to one quarter of the Kármán shedding period, T_K, when the flow is present. The plasma creates a

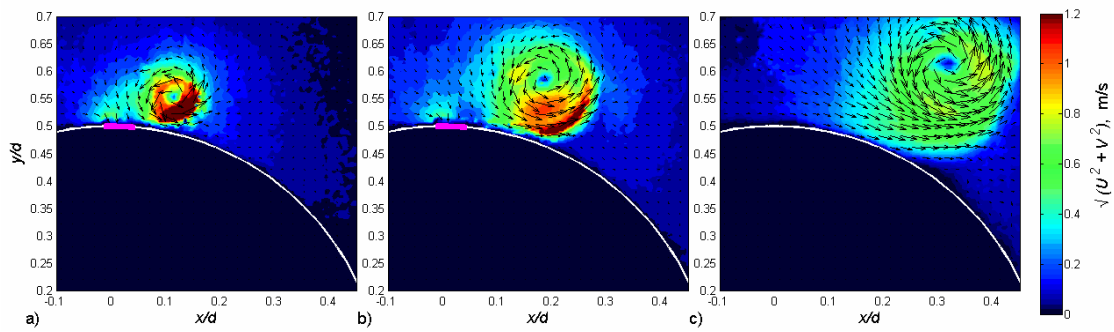

Figure 2. Instantaneous velocity magnitude induced by plasma in still air. Plasma activated for 33ms at f_{plasma} = 25kHz, E_{plasma} = ±3.5kV. (a): t = 8ms. (b): t = 24ms. (c): t = 56ms after plasma initiated. Plasma on during frames (a) and (b) with location as depicted in purple.

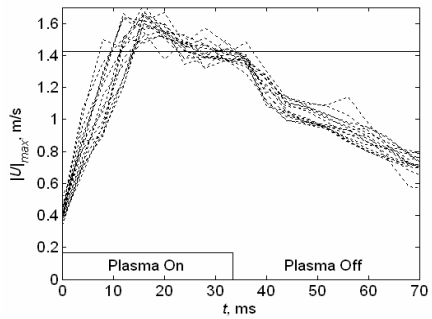

Figure 3. Maximum velocity magnitude induced by plasma in still air with time.

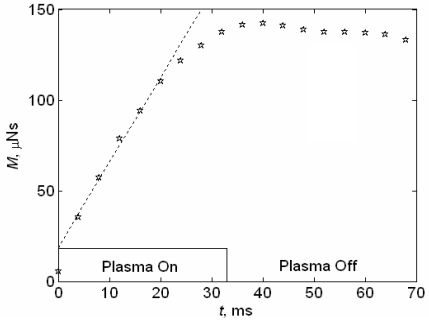

Figure 4. Total plasma-induced momentum in measurement region with time.

starting vortex which travels along the cylinder. Taking the characteristic plasma velocity, U_{plasma}, as the time-averaged peak velocity in the vortex after initiation ($7 \leq t \leq 33$ms) yields $U_{plasma}/U_\infty = 0.73$ (Fig. 3). Figure 4 shows the total momentum, M, added to the flow by the surface plasma with time. There is a reasonably linear increase, indicating that the plasma produces a constant body force whilst it is present. After the plasma switches off, there is a slow decrease due to viscous dissipation and transport out of the measurement area. Note that a significant portion of the induced flow is outside of the PIV image for $t > 24$ms, thus causing the non-linear increase after this time. The slope of the linear region yields the force produced by the plasma per unit width, F_{plasma} = 4.7mN/m. Expressed as a ratio of the dynamic force on the cylinder, $C_{plasma} = F_{plasma} / \frac{1}{2}\rho U_\infty^2 d = 0.041$.

3.2. FLOW FIELD WITHOUT PLASMA

The velocity profile in the wake of the circular cylinder without plasma is shown in Fig. 5. Six seconds of data were taken at 250Hz (1500 PIV image pairs), corresponding to approximately 47 vortex shedding cycles. The time-averaged profiles ((a) and (b)) exhibit symmetry along the horizontal axis, showing that the vortex shedding is equal from the top and bottom of the cylinder as expected. The wake region shows two mean recirculating cells centred at x/d = 1.25, y/d = ±0.25. Downstream of this region there is a sharp increase in velocity

fluctuations and mean velocity, indicating the onset of the Kármán vortex street. The position of maximum velocity fluctuations on the streamwise axis marks the length of the eddy formation region, $L_f/d = 1.92$ [2].

The roll-up of the upper shear layer into a large-scale Kármán vortex can be seen in the instantaneous vorticity profile in (c). In addition, small-scale roll-ups relating to the shear layer instability can be observed in the lower part of frame with spacing of $x/d \approx 0.3$. At this Reynolds number ($Re_d = 6{,}500$), the boundary layers remain laminar up to the separation point but the shear layers roll-up into transition eddies shortly after separation and before forming the Kármán vortex street [18]. Detailed study of the vortex shedding process was presented by Cantwell and Coles [3].

The Kármán shedding frequency and shear layer roll-up frequency were measured by taking the average velocity in the region $0.95 \leq x/d \leq 1.05$, $0.5 \leq y/d \leq 0.7$ (depicted in (c)). The Kármán shedding frequency, f_K, was clearly shown in the U-component time-trace since the shear layers waver back and forth throughout this region during the shedding cycle. The shear layer instability frequency, f_{SL}, was better shown in the V-component trace because the roll-ups rapidly switch from positive to negative V as the vortices pass through. The energy spectra for the two signals are shown in (d). Both show a peak at $f_K = 7.8$Hz, corresponding to $St_K = 0.206$. This compares very well to the data set of Roshko [14]. The V-velocity component spectrum shows a peak corresponding to $f_{SL} = 64.9$Hz ($St_{SL} = 1.71$), such that $f_{SL}/f_K = 8.3$, agreeing well with Prasad and Williamson [13].

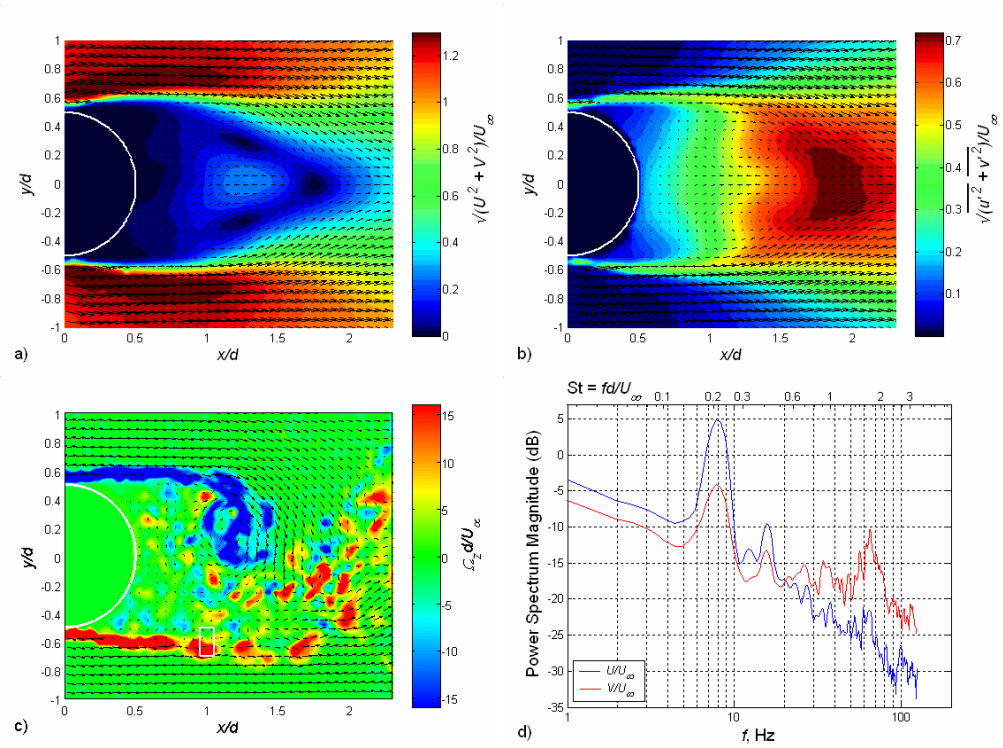

Figure 5. Flow field around the circular cylinder without plasma. (a): Time-averaged velocity magnitude over 47 shedding cycles. (b): Total turbulence profile. (c): Instantaneous vorticity profile. (d): Power spectrum based on measurements at $0.95 \leq x/d \leq 1.05$, $-0.7 \leq y/d \leq -0.5$.

3.3. EFFECT OF PLASMA ON THE CYLINDER WAKE

The effect of St_f on the wake behaviour was studied using two plasma actuators at a circumferential angle, $\theta = \pm 89°$. The plasma extended for an angle of approximately 7°, such that forcing occurs in the region $89° \leq \theta \leq 96°$. The profile of the body force throughout this region is not known, although it is expected to be strongest at the edge of the exposed electrode and decrease with θ. The two plasma actuators were either operated in phase (simultaneously) or 180° out of phase (oscillatory). In the oscillatory mode, the forcing frequency is defined as the reciprocal of the time between two occurrences of an electrode firing. Hence, exactly the same energy is expended for oscillatory and simultaneous modes at the same St_f. The pulsing was performed with both fixed plasma duration of 3ms ($0.025T_K$) and fixed duty cycle of 25%.

Figure 6 shows the velocity magnitude, turbulence level, and instantaneous vorticity profile at values of St_f for which four different wake regimes were observed. Firstly (Case A), the plasma causes two large-scale vortices to form on the top and bottom sides of the cylinder at the same time. This only occurred when the plasma actuators are fired together at $St_f = 0.2$ (Fig. 6 (a)). The two vortices are released together from the back of the cylinder and travel downstream as a counter-rotating vortex pair. This process occurs once every time the plasma fires (i.e. at the Kármán shedding frequency) and note that the vortices form much closer to the cylinder than without plasma (Fig. 5 (c)). The vortex pairs interact and mix chaotically downstream.

A quite different mode of shedding was observed when the plasma actuators were energised simultaneously at $St_f = 0.4$, or when oscillated at $St_f = 0.2$. In this second mode, Case B, the wake becomes hugely amplified with a vortex street that wavers dramatically back and forth. The amplification can be clearly seen in the diverging mean velocity field and increased velocity fluctuations in Fig. 6 (b). As with Case A, large scale vortices are formed quite close to the rear of the body, such that the formation region virtually vanishes. However, the vortices are now shed alternately from the lower and upper surfaces. Such a vortex can be seen in the instantaneous vorticity field, where a large-scale vortex shed from the top surface protrudes right across the wake. These vortices protrude to at least $y/d = -1$ within the measurement region, whilst it was rare to see a vortex cross beyond $y/d = -0.5$ without plasma. Also in Fig. 6 (b), it can be seen that the shear layer from the lower surface remains attached until quite close to the separation point on the opposite side of the cylinder. This amplified wake is expected to lead to rapidly fluctuating aerodynamic forces. Similar observation have been made by rotating a cylinder at $St_f = 0.2$ [8].

For $0.8 \leq St_f \leq 2.0$, a third mode of shedding is observed (Case C). In this regime, the Kármán vortex street is completely suppressed and a vortex is released from the top and bottom of the cylinder each time the plasma is activated. Thus, the frequency of these eddies increases with f_{plasma}. The eddies are smaller scale than the Kármán vortices and it is therefore likely that the

plasma is triggering roll-up of the shear layers. The train of vortices travel downstream at a shallow angle towards the centreline and combine after a short distance ($x/d \approx 2$). They then undergo mutual annihilation. This can be clearly seen in Fig. 6 (c), where two vortices of opposite sign appear on either side of the wake at the same distance downstream (simultaneous mode). Similar behaviour occurs with oscillatory plasma except that the chain of vortices is staggered. The velocity fluctuations are significantly reduced in this regime and the mean velocity shows a very short, thin and tapered wake region, as also observed by Thomas *et al*. [15]. Our observations show that the wake becomes less tapered as St_f increases so that the wake is shortest when $St_f = 0.8$-1.0 (c). It is likely that the drag is at a minimum at these frequencies.

At still higher forcing frequency ($St_f > 2.0$), the flow enters another flow regime: Case D. Here, the shear layers still roll-up at the plasma forcing frequency and separation is delayed, leading to a thinner wake (Fig. 6 (d)). However, the shear layers initially travel parallel to the free stream and start to form large-scale structures further downstream with similarity to the natural Kármán vortex street. The formation length is much longer than the canonical case so that the large-scale structures form quite close to the downstream edge of the measurement region. Hence, there is some uncertainty about the exact nature of this regime at present. It seems that at high St_f, the plasma only excites the shear layers near the cylinder with a largely undisturbed vortex street downstream.

In order to give a quantitative measure of the effectiveness of the plasma forcing, the momentum thickness of the cylinder wake, θ_{wake}, was calculated from the time-averaged streamwise velocity, $\overline{U}$, at $x/d = 2$ (Fig. 7):

$$\theta_{wake} = \int \frac{\overline{U}}{U_\infty}\left(1 - \frac{\overline{U}}{U_\infty}\right) dy \,. \tag{1}$$

Figure 8 shows that θ_{wake} increased by over 20% in the Case B flow regime ($St_f \leq 0.4$). In contrast, a broad plateau was observed within the Case C and D regimes, where θ_{wake} reduced by over 60% ($St_f \geq 0.8$). These are similar findings to those of Tokumaru and Dimotakis [16] for a rotationally oscillating cylinder, although note that the plasma induced velocity is lower than in their study ($U_{plasma}/U_\infty = 0.73$, as compared to $V_{r,max}/U_\infty = 2$) and the plasma only produces an effect in the region $89° \leq \theta \leq 96°$.

The wake behaviour in each regime was very similar regardless of whether the plasma was activated with constant duration or constant duty cycle. This would suggest that the shear layers are very sensitive to small disturbances at this actuator location, so that the flow control can be achieved with low power. This has huge implications for energy saving. For example, at $St_f = 0.2$ the power consumption is reduced by a factor of 10 between the two forcing modes (2.5% and 25% duty), yet the wake profile and momentum thickness is very similar (Fig. 8).

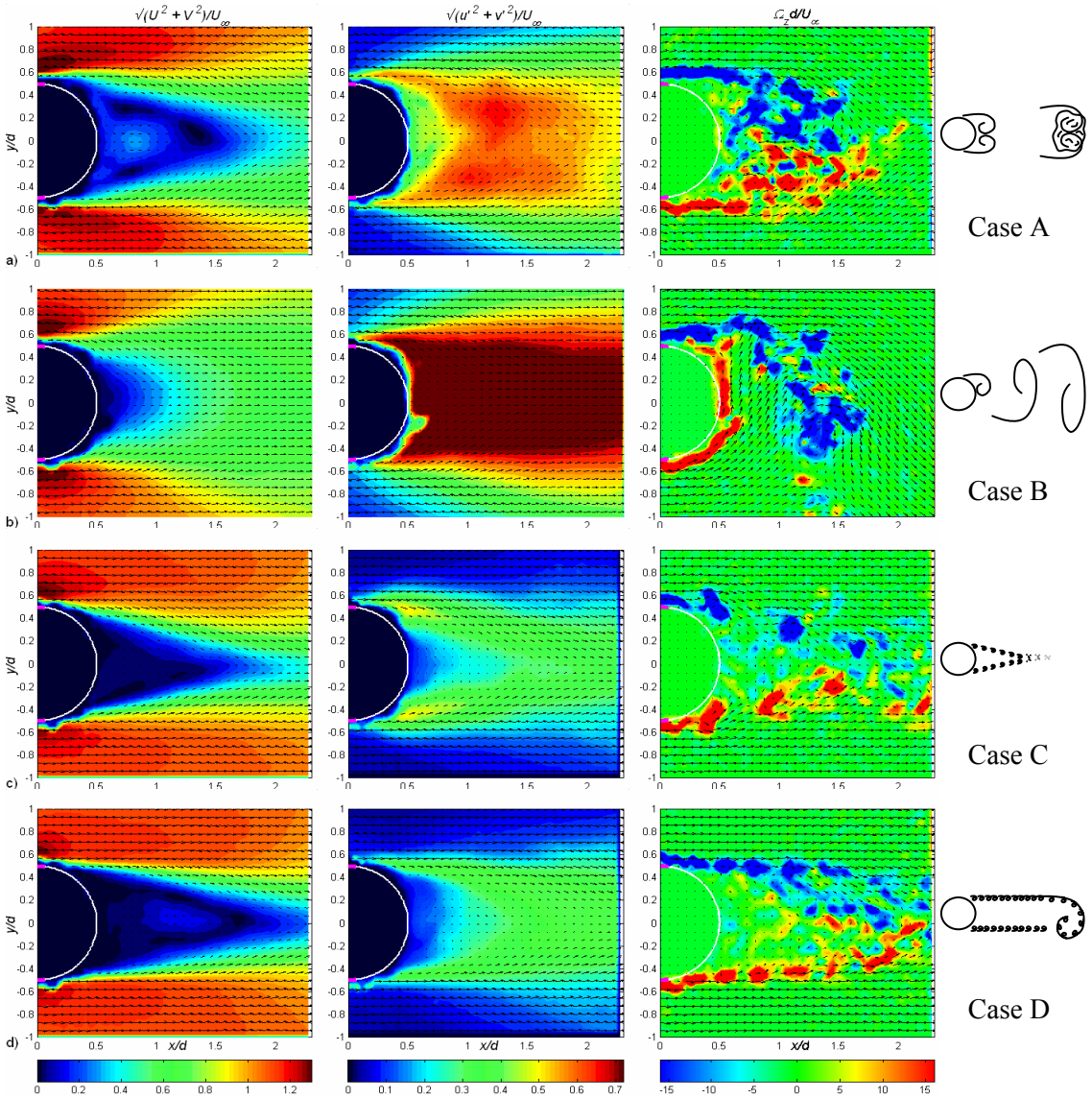

Figure 6. Flow field around the cylinder with plasma actuators at θ = ±89°. Time-averaged velocity magnitude after tU_∞/d = 80 (t = 2s, left column), total turbulence profile (middle) and instantaneous vorticity profile at tU_∞/d = 40 (right). (a): Electrodes actuated simultaneously at St_f = 0.2 (3ms, 2% duty). (b): Oscillatory actuation at St_f = 0.2 (3ms, 2% duty). (c): Simultaneous at St_f = 1.0 (3ms, 11% duty). (d): Simultaneous at St_f = 2.3, (3ms, 26% duty).

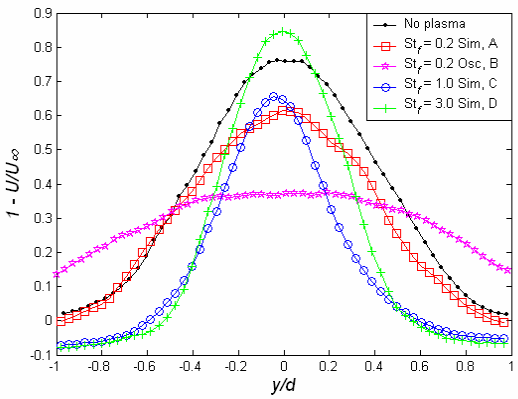

Figure 7. Wake velocity profile at x/d = 2 with plasma at θ = ±89° for various St_f.

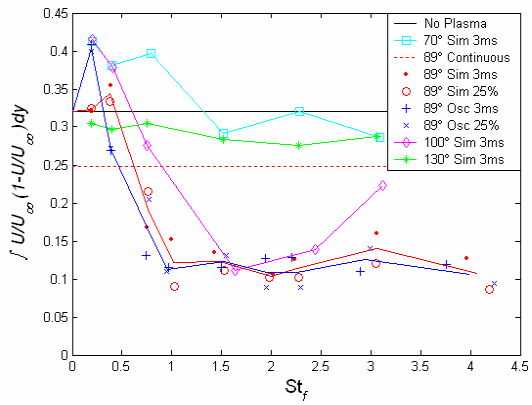

Figure 8. Momentum thickness at x/d = 2 for various St_f, θ, and actuation mode.

The effect of actuator location is also shown in Fig. 8. When the plasma was located upstream of the natural separation point (θ = ±70°), Case C behaviour could not be observed at any St_f. At high forcing frequency ($St_f > 1$) the shear layers did roll-up at f_{plasma}, but the Kármán vortex street and the wake profile remained similar to those without plasma. However at low forcing frequency, the amplification regime (Case B) was extended to $St_f \leq 0.8$, reflected by the increase in θ_{wake}. Thus the plasma can only act to amplify the Kármán vortex shedding when applied upstream of the separation point.

At θ = ±100°, the behaviour was similar to that at θ = ±89° except that there was less reduction in wake momentum thickness ($St_f \geq 0.8$), suggesting that the plasma was not as effective for flow control at this location. When the actuators were placed still further downstream (θ = ±130°), very little effect was observed. The plasma only weakly altered the recirculation in the wake region and did not affect the shear layers or the Kármán vortex shedding. The momentum thickness shows canonical values throughout the entire St_f range.

4. Conclusions

The near wake of a circular cylinder has been investigated using high-speed PIV in the subcritical regime (Re = 6,500). The flow was actively controlled using surface plasma actuators at θ = ±70−130° from the front stagnation point. Pulsed actuation was applied in the range $0.2 \leq St_f \leq 4.0$, with plasma forcing such that $U_{plasma}/U_\infty = 0.73$ and $C_{plasma} = 0.041$.
Four flow behaviours were observed, depending on St_f :

Case A – Two large scale vortices are shed simultaneously from the upper and lower sides of the cylinder. St_f = 0.2 (actuated simultaneously at θ = ±89°, only).

Case B – Amplification of the Kármán vortex street. $St_f \leq 0.4$.

Case C – Suppression of the Kármán vortex street. Shear layers roll-up at St_f and merge at $x/d \approx 2$. $0.8 \leq St_f \leq 2.0$.

Case D – Shear layers excited at St_f but form large-scale vortex street downstream. $St_f > 2.0$.

The wake became much wider in the Case B regime, with nearly 30% increase in turbulence intensity and 20% increase in wake momentum thickness. In contrast, the wake became much thinner in the Case C regime, where the turbulence intensity was reduced by 50% and the momentum thickness was reduced by over 60%. Flow control was most effective when θ = ±89° and we expect drag to be a minimum when $St_f \leq$ 0.8-1.0. Future work will consist of direct measurement of the dynamic lift and drag forces experienced by the cylinder.

Acknowledgements
EPSRC Research Grant (EP/D500850/1) and the use of the PIV system from the EPSRC Engineering Instrument Loan Pool are gratefully acknowledged.

References

1. Asghar, A., and Jumper, E. J., Phase Synchronization of Vortex Shedding from Multiple Cylinders Using Plasma Actuators, In: *41st Aerospace Sciences Meeting and Exhibit*, Reno, NV (2003) AIAA 2003-1028.
2. Bloor, M. S., and Gerrard, J. H., Measurements of Turbulent Vortices in a Cylinder Wake, *Proc. Royal Soc*. **A294** (1966) 319-342.
3. Cantwell, B., and Coles, D., An Experimental Study of Entrainment and Transport in the Turbulent Near Wake of a Circular Cylinder, *J. Fluid Mech*., **136** (1983) 321-374.
4. Cheng, M., Chew, Y. T., and Luo, S. C., Numerical Investigation of a Rotationally Oscillating Cylinder in Mean Flow, *J. Fluid. Struct*., **15** (2001) 981-1007.
5. Choi, S., Choi, H., and Kang, S., Characteristics of Flow Over a Rotationally Oscillating Cylinder at Low Reynolds Number, *Phys. Fluids*, **14** (8) (2002) 2767-2777.
6. Corke, T. C., and Post, M. L., Overview of Plasma Flow Control: Concepts, Optimization, and Applications, In: *43rd Aerospace Sciences Meeting*, Reno, NV (2005) AIAA 2005-0563.
7. Enloe, C. L., McLaughlin, T. E., VanDyken, R. D., Kachner, K. D., Jumper, E. J., Corke, T. C., Mechanisms and Responses of a Single Dielectric Barrier Plasma Actuator: Plasma Morphology, *AIAA J.*, **42** (3) (2004) 589-594.
8. Filler, J. R., Marston, P. L., and Mih, W. C., Response of the Shear Layers Separating from a Circular Cylinder to Small-Amplitude Rotational Oscillations, *J. Fluid Mech*., **231** (1991) 481-499.
9. Jukes, T. N., Choi, K.-S., Johnson, G. A., and Scott, S. J., Characterisation of Surface Plasma-Induced Wall Flows through Velocity and Temperature Measurement, *AIAA J.*, **44** (2006) 794-771.
10. Jukes, T. N., Choi, K.-S., Johnson, G. A., and Scott, S. J., Turbulent Drag Reduction by Surface Plasma through Spanwise Flow Oscillation, In: *3rd AIAA Flow Control Conference*, San Francisco, CA (2006) AIAA 2006-3693.
11. McLaughlin, T. E., Munska, M. D., Vaeth, J. P., Dauwalter, T. E., Goode, J. R., Siegel, S. G., Plasma-Based Actuators for Cylinder Wake Vortex Control, In: *2n AIAA Flow Control Conference*, Portland, OR (2004) AIAA 2004-2129.
12. Munska, M. D., and McLaughlin, T. E., Circular Cylinder Flow Control using Plasma Actuators, In: *43rd AIAA Aerospace Sciences Meeting and Exhibit*, Reno, NV (2005) AIAA 2005-141.
13. Prasad, A., and Williamson, C. H. K., The Instability of the Shear Layer Separating from a Bluff Body, *J. Fluid Mech*., **333** (1997) 375-402.
14. Roshko, A., On the Development of Turbulent Wakes from Vortex Streets, NACA Report 1191 (1954).
15. Thomas, F. O., Kozlov, A., and Corke, T. C., Plasma Actuators for Bluff Body Flow Control, In: *3rd AIAA Flow Control Conference*, San Francisco, CA (2006) AIAA 2006-2845.
16. Tokumaru, P. T., and Dimotakis, P. E., Rotary Oscillation Control of a Cylinder Wake, *J. Fluid Mech*., **224** (1991) 77-90.
17. Williamson, C. H. K., Vortex Dynamics in the Cylinder Wake, *Ann. Rev. Fluid. Mech.,* **28** (1996) 447-539.
18. Zdravkovich, M. M., Flow Around Circular Cylinders. Vol. 1: Fundamentals, Oxford University Press, (1997).